Alternative Substrate and Inhibition Kinetics of Aminoglycoside Nucleotidyltransferase 2″-I in Support of a Theorell–Chance Kinetic Mechanism†

Cynthia A. Gates‡ and Dexter B. Northrop*

Division of Pharmaceutical Biochemistry, School of Pharmacy, University of Wisconsin, Madison, Wisconsin 53706

Received August 13, 1987; Revised Manuscript Received January 15, 1988

ABSTRACT: Aminoglycoside nucleotidyltransferase 2″-I conveys multiple antibiotic resistance to Gram-negative bacteria because the enzyme adenylylates a broad range of aminoglycoside antibiotics as substrates [Gates, C. A., & Northrop, D. B. (1988) *Biochemistry* (preceding paper in this issue)]. The enzyme also catalyzes the transfer of a variety of nucleotides [Van Pelt, J. E., & Northrop, D. B. (1984) *Arch. Biochem. Biophys. 230*, 250–263]. This doubly broad substrate specificity makes it an excellent candidate for application of the alternative substrate diagnostic [Radika, K., & Northrop, D. B. (1984) *Anal. Biochem. 141*, 413–417] as a means to determine its kinetic mechanism. The kinetic patterns presented here are composed of one set of intersecting lines and one coincident line and are consistent with a Theorell–Chance kinetic mechanism in which nucleotide binding precedes aminoglycosides, pyrophosphate is released prior to the nucleotidylated aminoglycoside (Q), and turnover is controlled by the rate-limiting release of the final product. Substrate inhibition by tobramycin (B) is partial and uncompetitive versus Mg–ATP, indicating that B binds to the EQ complex, but not in the usual dead-end fashion common to an ordered sequential release of products; instead, Q may escape from the abortive EQB complex at a finite rate. Dead-end inhibition by neomycin C (I) is also partial and uncompetitive versus Mg–ATP but is slope-linear, intercept-hyperbolic, partial noncompetitive versus gentamicin A; both kinetic patterns signify the formation of a partial abortive EQI complex. In a new and complex form of multiple inhibition, the substrate inhibition constant of tobramycin increases with increasing concentrations of the dead-end inhibitor, signifying competition for EQ; but surprisingly, the dead-end inhibitor activates the substrate-inhibited enzyme at high concentrations, consistent with a more rapid escape of Q from EQI than from EQB. Product inhibition by AMP–tobramycin is noncompetitive versus Mg–ATP and uncompetitive versus tobramycin; in the latter, the substrate inhibition constant increases with increasing concentrations of product, signifying the formation of an EQQ complex. Moreover, the lack of enhancement of substrate inhibition at moderate concentrations of added product confirms that the enzyme exists primarily as the EQ complex during normal turnover.

Aminoglycoside nucleotidyltransferase 2″ [ANT(2″)-I] (EC 2.7.7.46) is one of many enzymes that confer antibiotic resistance to Gram-negative bacteria harboring R factors. In addition to O-nucleotidylation, there are enzymes that acetylate the amino groups (acetyltransferases) and others that phosphorylate hydroxyl groups (phosphotransferases) of aminoglycosides. In spite of potential nephro- and ototoxicity, aminoglycoside antibiotics are a mainstay of contemporary antibiotic therapy since they exhibt rapid bactericidal activity against a broad range of microorganisms, including many Gram-negative aerobic bacteria (Norris & Raudin, 1984; Pelletier, 1985). The presence of one or more aminoglycoside-modifying enzymes, most of which have a broad range of substrate specificity (Radika & Northrop, 1984a; Williams & Northrop, 1978), greatly reduces the efficacy of antibiotics in clinical pathogens.

Of all the aminoglycoside-modifying enzymes, only the acetyltransferase enzymes (AAC) have been the subject of extensive kinetic analyses. Aminoglycoside acetyltransferase (3)-I was found to follow a random kinetic mechanism on the basis of patterns of initial velocity, product inhibition, and dead-end inhibition (Williams & Northrop, 1978). Similarly, the bifunctional AAC(6′)–APH(2″) enzyme from *Staphylococcus aureus* was shown to follow a random mechanism (Martel et al., 1983). Purified AAC(6′)-IV was subjected to kinetic analysis by using a variety of antibiotics and coenzymes which led to a detailed structure–activity analysis (Radika & Northrop, 1984a). In addition, by exploiting the ability of AAC(6′)-IV to accept a variety of aminoglycosides and coenzymes as substrates, Radika and Northrop (1984b) developed a kinetic protocol in which the concentration of one substrate is varied in the presence of fixed and saturating concentrations of structural variants or alternatives of a second substrate. Unique pairs of patterns for each of the major classes of kinetic mechanisms were found by using this method. Application of this alternative substrate diagnostic to AAC(6′)-IV revealed a rapid-equilibrium random kinetic mechanism in which catalysis is the rate-limiting segment (Radika & Northrop, 1984c).

In the 15 years since the discovery of ANT(2″)-I, only one study of the kinetic mechanism of this enzyme has been described. On the basis of two initial velocity patterns, product inhibition by pyrophosphate and dead-end inhibition of triphosphate, Lombardini and Cheng-Chu (1984) surmised that ANT(2″)-I followed an ordered, sequential kinetic mechanism in which the nucleotide substrate binds prior to the antibiotic, but the order of product release was not ventured, and enzyme activity was quantitated by measuring the incorporation of radiolabeled nucleotide into the polycationic product. Gold-

† This investigation was supported in part by Research Grant AI1106 from the National Institutes of Health (1979–1984) and in part by the Graduate School of the University of Wisconsin. D.B.N. is the recipient of Career Development Award GM00254 from the National Institutes of Health. Preliminary reports have appeared (Gates & Northrop, 1984, 1985).

* Author to whom correspondence should be addressed.

‡ Present address: Department of Biochemistry, University of Wisconsin, Madison, WI 53706.

0006-2960/88/0427-3826$01.50/0

man and Northrop (1976) reported a lack of linearity of this assay with respect both to time and enzyme concentration. Lombardini and Cheng-Chu achieved linearity by restricting assays to conditions of low concentrations of both nucleotide and antibiotic, which precluded accurate detection of intercept effects in kinetic patterns.

Because ANT(2″)-I is capable of accepting a large number of both nucleotide triphosphates and aminoglycosides as substrates (Van Pelt & Northrop, 1984; Gates & Northrop, 1988a), it is an ideal candidate for application of the alternative substrate diagnostic. The present report describes the results of the alternative substrate diagnostic plus substrate, dead-end, and product inhibition kinetics which confirm the substrate binding order of Lombardini and Cheng-Chu, establish the order of product release, suggest the identity of the rate-limiting segment of catalytic turnover, and support a Theorell–Chance kinetic mechanism for ANT(2″)-I.

Experimental Procedures

Materials. Gentamicins C_1, C_{1a}, and A sulfate and sisomicin sulfate were the gifts of Dr. George Miller, Schering Corp. Tobramycin was the gift of Dr. Marvin Gorman of Lilly Research Laboratories. Neomycin C was the gift of Dr. Joseph Grady, Upjohn Chemical Co. Tobramycin–AMP was the gift of Dr. Jean Van Pelt and Dr Perry Frey, Enzyme Institute, University of Wisconsin—Madison. *Escherichia coli* W677/pMY10 was provided by M. Yagisawa of Julian Davies' laboratory. Magnesium acetate was purchased from Baker Chemical Co. All other biochemicals were purchased from Sigma Chemical Co. Two electrophoretic variants of aminoglycoside nucleotidyltransferase were purified 43- and 85-fold from *E. coli* W677/pMY10 by a modification of the method of Van Pelt and Northrop (1984). Enzyme preparations that had specific activities ranging from 1.1 to 2.2 international units (IU)/mg in the standard assay at pH 9.1 were used in kinetic studies.

Enzyme Assays. Aminoglycoside nucleotidyltransferase activity was measured by a modification of the coupled enzyme assay of Van Pelt and Northrop (1984) which links the reaction catalyzed by ANT(2″) to UDP-glucose pyrophosphorylase, phosphoglumutase, and glucose-6-phosphate dehydrogenase reactions. The rate of increase of absorbance of NADPH at 340 nm was monitored continuously under conditions described in the preceding paper in this issue (Gates & Northrop, 1988a).

Data Analysis. Kinetic data dependent upon varied concentrations of substrate were fitted to eq 1 and 2, representing the absence and presence of substrate inhibition, respectively.

$$v = VA/(K_a + A) \quad (1)$$

$$v = VA/(K_a + A + A^2/K_I) \quad (2)$$

Patterns of data obtained in the presence of added inhibitor were initially examined by fitting data from each concentration of inhibitor to these same equations. To determine the form of inhibition, replots of slopes and intercepts were examined graphically, and the apparent V and V/K values were fitted to eq 3 and 4, respectively, weighted by the standard deviations

$$V_i = V_0/(1 + I/K_{ii}) \quad (3)$$

$$V_i/K_a = V_0/K_a(1 + I/K_{is}) \quad (4)$$

obtained from the primary regression. Apparent maximal velocities generating a hyperbolic replot were fit to eq 5. To obtain inhibition constants, data from patterns were then fit

$$V_i = V_0(1 + I/K_{id})/(1 + I/K_{ii}) \quad (5)$$

Table I: Gentamicin C_1 Kinetic Constants at Fixed Concentrations of Alternative Nucleotides

V (IU/mg)	V/K (L mg^{-1} min^{-1})	nucleotide[a]	concn (mM)
5.57 ± 0.11	0.38 ± 0.01	Mg–ATP	11.32
2.89 ± 0.07	0.38 ± 0.02	Mg–dATP	2.42
2.30 ± 0.07	0.050 ± 0.002	Mg–dGTP	0.67

[a] Relative values of V of alternative nucleotides are 5:2:1 and of V/K are 1:2.7:4, respectively.

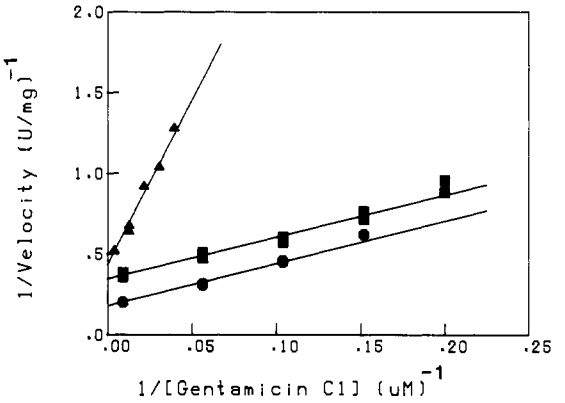

FIGURE 1: Alternative substrate diagnostic with gentamicin C_1 as the variable substrate. The alternative nucleotide substrates were Mg–ATP (●) at 11.3 mM, Mg–dATP (■) at 2.4 mM, or Mg–dGTP (▲) at 0.7 mM. The solid lines are drawn from the data fit to eq 1. The concentration range of gentamicin C_1 was from 6.6 μM with Mg–ATP, 5.0–112.4 μM for Mg–dATP, and 25.3–253.0 μM for Mg–dGTP. The free Mg^{2+} concentration was fixed at 10.0 mM.

to one of the following rate equations, as indicated in Table III:

$$v = VA/[K_a + A(1 + I/K_{ii})] \quad (6)$$

$$v = VA/[K_a(1 + I/K_{is}) + A(1 + I/K_{ii})] \quad (7)$$

$$v = VA/[K_a + A(1 + I/K_{ii})/(1 + I/K_{id})] \quad (8)$$

$$v = VA/[K_a(1 + I/K_{is}) + A(1 + I/K_{ii})/(1 + I/K_{id})] \quad (9)$$

$$v = VA/[K_a(1 + I/K_{is}) + A(1 + A/K_I)] \quad (10)$$

$$v = VA/[K_a + A(1 + I/K_{ii} + A/K_I)] \quad (11)$$

In these equations, v is a measured velocity, V is a maximal velocity, A is a concentration of antibiotic or nucleotide, K_a is a Michaelis–Menten constant for antibiotic or nucleotide, I is a concentration of inhibitor, K_I is a substrate inhibition constant, K_{is} is the slope inhibition constant, and K_{ii} and K_{id} are intercept inhibition constants. Linear data were fitted to

$$y = mx + b \quad (12)$$

where m is the slope and b is the intercept. All data were fitted on a NorthStar Horizon computer using the BASIC program of Duggleby (1984).

Results

Patterns of Alternative Substrates. The kinetic constants of gentamicin C_1 were determined in the presence of saturating concentrations of Mg–ATP, Mg–dATP, or Mg–dGTP. Apparent values of V and V/K for the single aminoglycoside vary by factors of 2.5 and 7.6, respectively, as listed in Table I. The resulting pattern of intersecting lines is illustrated in Figure 1. The values of V and V/K for each of the alternative nucleotides used in the diagnostic themselves differed by about 5-fold.

The kinetic constants of Mg–ATP were similarly determined with gentamicin A, C_1, or C_{1a} as the alternative substrate. As

Table II: Mg–ATP Kinetic Constants at Fixed Concentrations of Alternative Antibiotics[a]

Mg–ATP			
V (IU/mg)	V/K (L mg^{-1} min^{-1})	antibiotic[b]	concn (μM)
6.7 ± 0.1	3.7 ± 0.1	gentamicin A	1020.0
6.8 ± 0.1	3.5 ± 0.1	gentamicin C_1	249.6
3.1 ± 0.05	6.5 ± 0.3	gentamicin C_{1a}	5.9

[a] Reaction velocities were measured spectrophotometrically in 1-cm cells with gentamicin A or C_1 or in 5-cm cuvettes with gentamicin C_{1a}. [b] Relative values of V when antibiotic is varied are 1.5:8.9:1 and of V/K are 1:7.2:119, respectively.

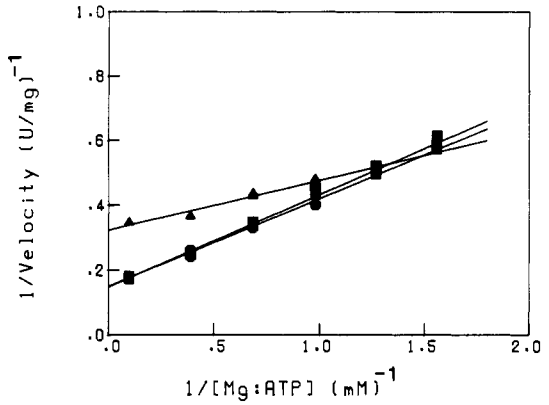

FIGURE 2: Alternative substrate diagnostic with Mg–ATP as the variable substrate. The alternative aminoglycoside substrates were gentamicin A (●) at 1020.0 μM, gentamicin C_{1a} (■) at 249.6 μM, and gentamicin C_1 (▲) at 5.9 μM. The solid lines represent the data fit to eq 1. The concentration range of Mg–ATP was from 0.64 to 10.21 mM; the concentration of free Mg ion was fixed at 10 mM for each total nucleotide concentration. Kinetic constants for the nucleotide with gentamicin C_{1a} as the alternative substrate were determined with 5-cm path length cuvettes, whereas those determined with gentamicin A or C_1 used assays performed in 1-cm path length cuvettes.

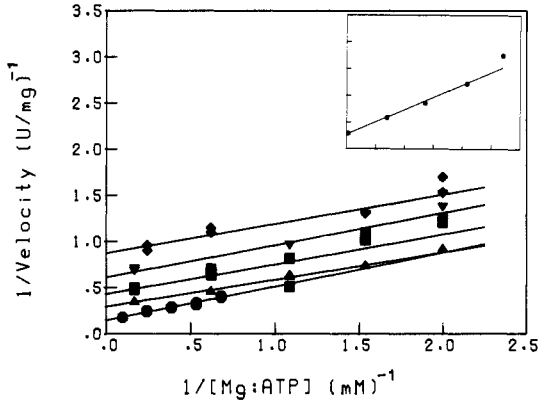

FIGURE 3: Uncompetitive substrate inhibition by sisomicin with Mg–ATP as the variable substrate. Each solid line represents the data fit to eq 1. The concentrations of sisomicin were 0.03 mM (●), 0.70 mM (▲), 1.36 mM (■), 2.08 mM (▼), and 2.70 mM (♦). The Mg–ATP concentration ranges were from 1.46 to 10.24 mM for 0.03 mM sisomicin and from 0.5 to 6.0 mM for 0.70, 1.26, 2.08, and 2.70 mM sisomicin. The free Mg^{2+} ion concentration was fixed at 10 mM for each nucleotide concentration. Inset: Intercept replot for Mg–ATP versus sisomicin. The solid line represents the fit of the apparent $1/V_{max}$ values of Mg–ATP to eq 3.

shown in Table II, values of V and V/K for the nucleotide are identical with gentamicin A or C_1 as an alternative substrate but differ by about 2-fold with gentamicin C_{1a}. As a point of reference, the values of V/K for each of the alternative aminoglycoside substrates themselves differed by about 120-fold. The resulting pattern is illustrated in Figure 2 and appears to be composed of two coincident lines and one very closely intersecting line.

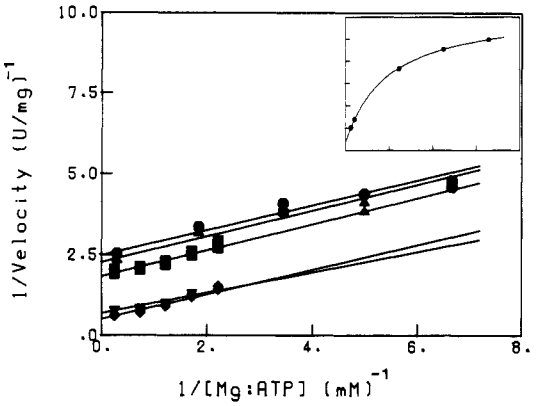

FIGURE 4: Uncompetitive substrate inhibition by tobramycin with Mg–ATP as the variable substrate. Each solid line was drawn from the data fit to eq 1. The concentrations of tobramycin were 0.06 mM (♦), 0.10 mM (▼), 0.61 mM (■), 1.12 mM (▲), and 1.64 mM (●). The Mg–ATP concentration ranges were from 0.45 to 4.10 mM for 0.06 and 0.10 mM tobramycin and from 0.15 to 3.41 mM for 0.61, 1.12, and 1.64 mM tobramycin. The free Mg^{2+} ion concentration was fixed at 10.0 mM for each total nucleotide concentration. Inset: Intercept replot of Mg–ATP versus tobramycin. The solid line represents the fit of the apparent $1/V_{max}$ values of Mg–ATP to eq 5.

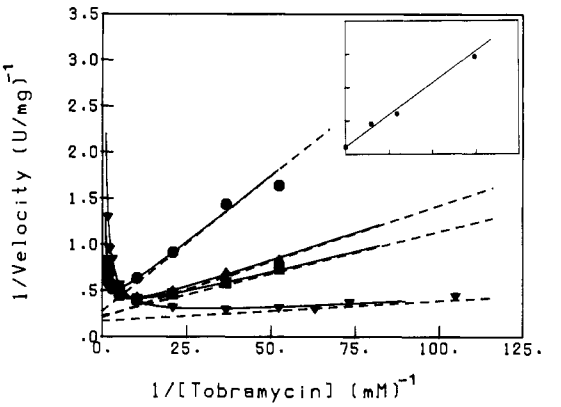

FIGURE 5: Inhibition by neomycin C with tobramycin as the variable substrate. Each curved, solid line represents the data fit to eq 2, and each dashed line designates the position of $1/V_{max}$ and K/V. The concentrations of neomycin C were 0 mM (▼), 0.12 mM (■), 0.24 mM (▲), and 0.59 mM (●), giving respectively 87 ± 19, 228 ± 34, 249 ± 28, and 578 ± 83 μM as values for substrate inhibition constants of tobramycin. The concentration ranges of tobramycin were from 0.010 to 0.610 mM for 0 mM neomycin C and from 0.019 to 0.610 mM for 0.12, 0.24, and 0.59 nM neomycin C. Mg–ATP and free Mg^{2+} were fixed at 11.86 and 10 mM, respectively. Inset: Slope replot of tobramycin versus neomycin C. The solid line is drawn from a fit of apparent K/V values of tobramycin to eq 4.

Patterns of Dead-End Inhibition. The form of substrate inhibition by aminoglycosides was determined by varying the concentration of the noninhibitory substrate, Mg–ATP, in the presence of fixed and saturating concentrations of sisomicin or tobramycin. A parallel inhibition pattern with a linear effect on intercepts was obtained with sisomicin, as shown in Figure 3, indicative of normal uncompetitive substrate inhibition. A parallel inhibition pattern was also obtained with tobramycin, but with a hyperbolic replot of intercepts as shown in Figure 4, indicative of partial uncompetitive substrate inhibition. The form of dead-end inhibition by an aminoglycoside analogous to substrates was examined as a function of the concentrations of both aminoglycoside and nucleotide substrates. An intersecting inhibition pattern with a linear replot of slopes was obtained with neomycin C when tobramycin was the varied substrate, as shown in Figure 5. There may be a small effect on intercepts, but it is obscured by intense substrate inhibition. Using gentamicin A, which does not give substrate inhibition,

Table III: Inhibition Constants of Aminoglycosides

inhibitor	substrate	pattern[a]	eq	K_{is} (μM)	K_{ii} (μM)	K_{id} (μM)
sisomicin	Mg–ATP	UC	6		0.65 ± 0.03	
tobramycin	Mg–ATP	p-UC	8		0.051 ± 0.01	0.74 ± 0.17
neomycin C	gentamicin A	p-NC	9	0.051 ± 0.004	0.10 ± 0.01	0.48 ± 0.16
neomycin C	Mg–ATP	p-UC	8		0.092 ± 0.009	0.95 ± 0.30
neomycin C	tobramycin	C	10	0.031 ± 0.01		
AMP–tobramycin	Mg–ATP	NC	7	0.42 ± 0.20	0.31 ± 0.04	
AMP–tobramycin	tobramycin	UC	11		0.17 ± 0.02	

[a] C, competitive; NC, noncompetitive; UC, uncompetitive; p, partial.

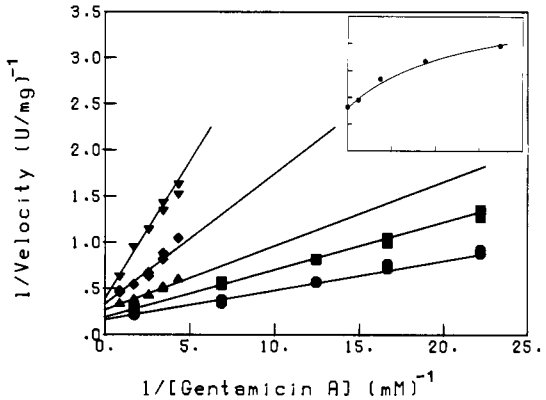

FIGURE 6: Noncompetitive inhibition by neomycin C with gentamicin A as the variable substrate. Each solid line represents the data fit to eq 1. The concentrations of neomycin were 0 mM (●), 0.025 mM (■), 0.075 mM (▲), 0.177 mM (♦), and 0.348 mM (▼). The concentration ranges of gentamicin A were from 0.045 to 0.580 mM for 0 and 0.025 mM gentamicin A and from 0.230 to 1.155 mM for 0.075, 0.177, and 0.348 mM gentamicin A. The Mg–ATP and free Mg^{2+} ion concentrations were fixed at 10.24 and 10 mM, respectively. Inset: Intercept replot of gentamicin A versus neomycin C. The solid line represents the fit of apparent $1/V_{max}$ values of gentamicin A to eq 5.

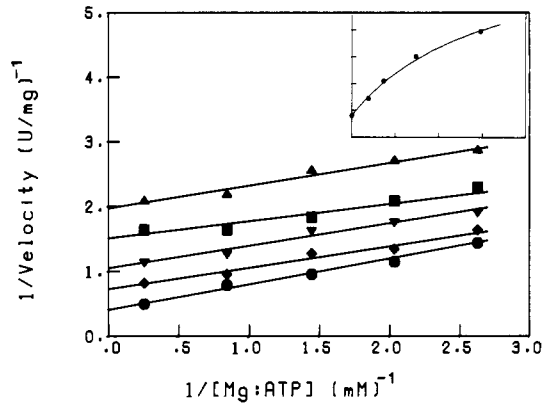

FIGURE 7: Uncompetitive inhibition by neomycin C with Mg–ATP as the variable substrate. Each solid line is drawn from the data fit to eq 1. The concentrations of neomycin C were 0 mM (●), 0.08 mM (♦), 0.15 mM (▼), 0.30 mM (■), and 0.59 mM (▲). The concentration range of Mg–ATP was 0.38–3.94 mM; free Mg^{2+} ion concentration was fixed at 10 mM for each total nucleotide concentration. The concentration of gentamicin A was fixed at 0.22 mM. Inset: Intercept replot of Mg–ATP versus neomycin C. The solid line represents the fit of apparent $1/V_{max}$ values of Mg–ATP to eq 5.

an intersecting inhibition pattern with a linear replot of slopes was obtained also, but with a hyperbolic intercept effect as shown in Figure 6. This pattern is one form of partial mixed inhibition because the linear slope effect and hyperbolic intercept effect clearly derive from different origins. Neomycin C gives a parallel inhibition pattern versus Mg–ATP, also with hyperbolic intercepts, shown in Figure 7. The neomycin C inhibition pattern is partial uncompetitive inhibition.

Patterns of Product Inhibition. Only the nucleotidylated aminoglycoside was studied as a product inhibitor, as the other product, pyrophosphate, was consumed and monitored in the spectrophotometric assay. An intersecting pattern with a linear replot of intercepts but an uncertain replot of slopes was obtained with tobramycin–AMP when Mg–ATP served as the variable substrate, as shown in Figure 8 and tentatively described as normal noncompetitive inhibition. The pattern appears parallel versus tobramycin concentrations, as shown in Figure 9, but the presence or absence of a weak slope effect is obscured by substrate inhibition. The pattern gives a linear replot of intercepts consistent with normal uncompetitive inhibition.

The kinetic constants of inhibition are listed in Table III. These were obtained by fitting complete patterns of data to the appropriate rate equation, discerned by analysis of the slope and intercept replots described above. Because some patterns and equations are unusual, both are identified together with the inhibition constants.

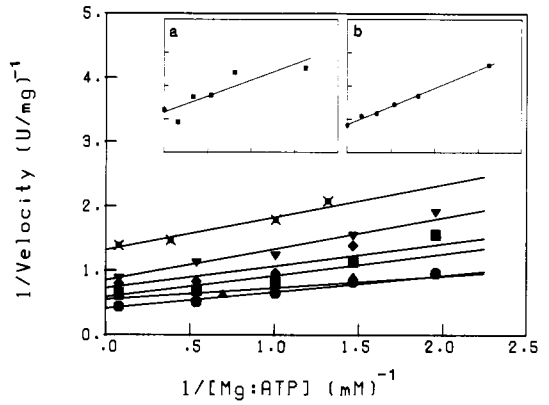

FIGURE 8: Noncompetitive inhibition by tobramycin–AMP with Mg–ATP as the variable substrate. Each solid line represents the data fit to eq 1. The concentrations of tobramycin–AMP were 0 mM (●), 0.065 mM (▲), 0.135 mM (■), 0.216 mM (♦), 0.325 mM (▼), and 0.650 mM (×). The concentration ranges of Mg–ATP were 0.51–12.86 mM for 0.065, 0.135, 0.216, and 0.325 mM tobramycin–AMP and 0.76–12.86 mM for 0.650 mM tobramycin–AMP. Free Mg^{2+} ion concentration was fixed at 10 mM for each total nucleotide concentration. Tobramycin was fixed at 0.06 mM. Inset a: Slope replot of Mg–ATP versus tobramycin–AMP. The solid line represents the fit of apparent K/V values of Mg–ATP to eq 4. Inset b: Intercept replot of Mg–ATP versus tobramycin–AMP. The solid line is drawn from the fit of apparent $1/V$ values of Mg–ATP to eq 3.

Discussion

Kinetics of Substrates. Because aminoglycoside nucleotidyltransferase 2″-I accepts such a large number of aminoglycoside and nucleotide substrates, it is an ideal candidate for alternative substrate kinetics. This was fortunate because, given micromolar kinetic constants plus limitations of a multiple-linked enzymatic assay, ANT(2″)-I is a very poor candidate for kinetic analysis on the basis of initial velocities. The aminoglycosides and nucleotides selected as alternative substrates had large differences in V/K, which ensured that kinetic differences of each alternative substrate had a potential

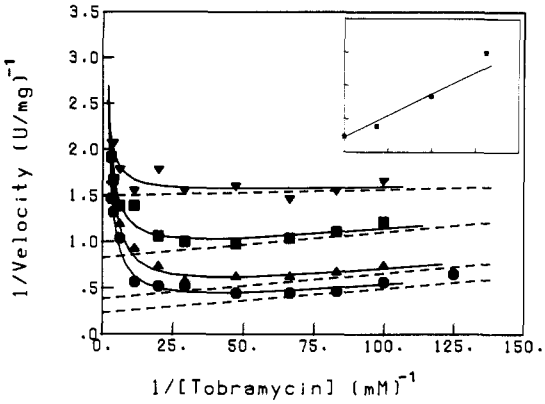

FIGURE 9: Uncompetitive inhibition by tobramycin–AMP with tobramycin as the variable substrate. Each curved, solid line represents the data fit to eq 2, and each dashed line notes the position of K/V and $1/V$. The concentrations of tobramycin–AMP were 0 mM (●), 0.15 mM (▲), 0.40 mM (■), and 0.65 mM (▼), giving respectively 56 ± 17, 81 ± 24, 235 ± 62, and 792 ± 268 μM as values for substrate inhibition constants of tobramycin. The concentration range of tobramycin was 0.008–0.326 mM for 0 mM tobramycin–AMP and 0.01–0.326 mM for 0.15, 0.40, and 0.65 mM tobramycin–AMP. Mg–ATP and free Mg^{2+} concentrations were fixed at 12.86 and 10 mM, respectively. Inset: Intercept replot of tobramycin versus tobramycin–AMP. The solid line is drawn from the fit of apparent $1/V_{max}$ values of tobramycin to eq 3.

for expression in the kinetics of the varied substrate. These differences were clearly expressed in the intersecting pattern of Figure 1. The changes in V/K_b of gentamicin are of the same magnitude as the differences in values of V/K_a for each of the alternative nucleotide substrates (Table I). These changes are associated with either a random sequential or an ordered sequential (with nucleotide binding first) kinetic mechanism (Radika & Northrop, 1984b).

Similar changes were not expressed, however, in Figure 2. The V/K of Mg–ATP changes in one case by only about 2-fold (Table II), in contrast to the 119-fold difference in the values of V/K_a for alternative gentamicins. This disparity suggests that the origin of the singular change in slope is other than those discussed by Radika and Northrop,[1] who note that an absence of a slope effect in one of the two patterns is associated with an ordered sequential addition of substrates. The 2.2-fold difference in intercept is equally insignificant against the much larger difference in kinetic constants which indicates a Theorell–Chance kinetic mechanism. Therefore, the kinetic mechanism is as follows: nucleotide binds to ANT(2″)-I first, followed by aminoglycoside; after catalysis, pyrophosphate is released first, followed by the nucleotidylated aminoglycoside;

Scheme I: Substrate Inhibition

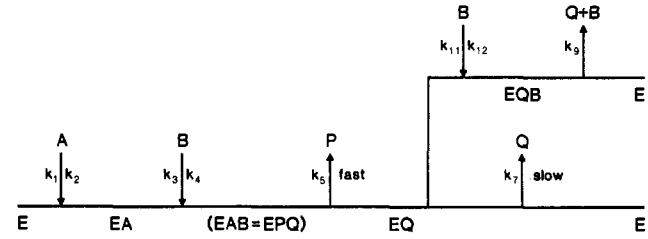

although central complexes obviously exist (as indicated by differences in values of V/K_b), they are kinetically insignificant with respect to catalytic turnover.

Sequential kinetic mechanisms for enzymes catalyzing the reaction of two substrates obey the initial velocity equation:

$$\frac{v}{E_t} = \frac{VAB}{K_bA + K_aB + K_{ia}K_b + AB} \quad (13)$$

Equation 13 has the same general form for all three sequential mechanisms discussed above. For a Theorell–Chance kinetic mechanism, the origins of kinetic constants are as follows: V/K_a is determined by the binding of nucleotide, substrate A; V/K_b consists of the binding of aminoglycoside, substrate B, plus catalysis and the release of pyrophosphate, product P; and V is determined solely by the release of the nucleotidylated aminoglycoside, product Q.

Kinetics of Substrate Inhibition. Uncompetitive substrate inhibition by aminoglycosides versus Mg–ATP (Figure 3) is consistent with secondary binding of the inhibitory substrate to the enzyme–AMP–aminoglycoside complex (EQ) to form a dead-end complex, because EQ is the only form of enzyme isolated from the binding of Mg–ATP by irreversible steps (Cleland, 1979). Moreover, binding of aminoglycosides to this form of enzyme requires that the AMP–aminoglycoside be released in a predominantly ordered series of three steps: (a) the release of the aminoglycoside portion of Q, (b) a slow conformational change, and (c) the release of the AMP portion [see the following paper in this issue (Gates & Northrop, 1988b)]. The first step exposes the specific binding site to allow binding of a second molecule of aminoglycoside to the enzyme. It must be followed by a slow step in order for this particular form of enzyme to accumulate during turnover to allow inhibition to occur at concentrations of aminoglycoside only slightly above Michaelis levels. Binding of B to EQ must also prevent the release of the AMP portion of Q if it is to cause dead-end inhibition; therefore, the slow step must include a conformational change which controls the release of nucleotide.[2] Because the uncompetitive substrate inhibition is partial, however, the ability of aminoglycosides to trap the second product must be incomplete.[3] Partial inhibition re-

[1] For example, Radika and Northrop note in their fourth caveat that the unique diagnostic pattern of Theorell–Chance kinetic mechanisms assumes that the structural changes associated with alternatives of B (B′ etc.) are carried into product P, and not to Q; thus, the maximal velocity is not affected by a change in B because it is solely dependent upon the rate of release of Q. However, during turnover of ANT(2″)-I, no part of B (aminoglycoside) appears in P (pyrophosphate) but B does contribute substantially to Q (nucleotidylated aminoglycoside). Thus, the small intercept effect in Figure 2 may originate from a difference in the rate of release of the gentamicin C_{1a} portion of Q. Consistent with this hypothesis is a lower dissociation constant of gentamicin C_{1a} from its EQB complex, as expressed in its substrate inhibition constant (Gates & Northrop, 1988a). The small change in slope may originate from a small (i.e., not more than 1–2%) amount of randomness in the mechanism, which would go undetected in initial velocity patterns. Alternatively, aminoglycoside impurities may be present in gentamicin C_{1a}. Marti and Northrop (unpublished results) have noted biphasic kinetics in the reaction of 3N-aminoglycoside acetyltransferase I with gentamicin C_{1a} and have resolved two components on ion pair reversed-phase high-pressure liquid chromatography which do not resolve during ion-exchange chromatography.

[2] Also, it is unlikely that the rate of dissociation of nucleotide from the enzyme could be slow enough to dominate catalytic turnover by itself (and if it did, all values of V would be the same with different antibiotics), so it is reasonable that it is preceded by a slow step. If B can trap the product nucleotide in the EQB complex, it follows that B probably can trap substrate nucleotide in the EAB complex; hence, uncompetitive aminoglycoside substrate inhibition contributes to a confirmation of the ordered binding of substrates.

[3] A finite release of Q from EQB also indicates that some randomness in the order of release of the aminoglycoside and nucleotide portions of Q should exist, allowing for an alternative reaction pathway in which the release of the AMP portion precedes that of the aminoglycoside portion. This is a minor reaction pathway, however, because a comparison of the vertical intercept to the horizontal asymptote of the inset of Figure 4 shows that the escape of the AMP portion of Q when the aminoglycoside site is occupied could contribute no more than 5% to the catalytic turnovers employing tobramycin.

Scheme II: Dead-End Inhibition

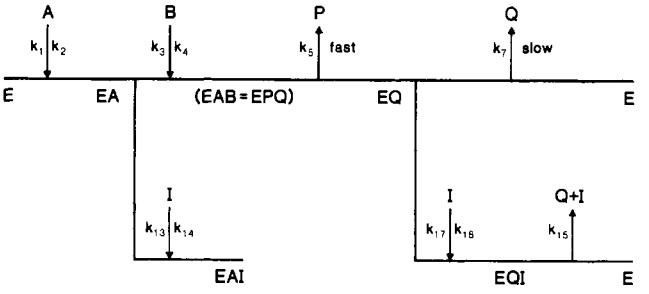

quires a finite release of Q from EQB as illustrated in Scheme I and described by the equation:

$$\frac{v}{E_t} = \frac{VAB}{K_bA + K_aB + K_{ia}K_b + \dfrac{AB(1 + B/K_{bi})}{1 + B/K_{bd}}} \quad (14)$$

The derivation of this equation assumed that the binding of B to EQ was in rapid equilibrium. That this is a valid assumption is confirmed by the effects of viscosity and pH on the kinetic parameters of ANT(2″)-I (see the following paper in this issue) and by the results of multiple product and dead-end inhibition (see below). K_{bi} is thus a true dissociation constant of B from EQ and is defined as k_{12}/k_{11}. K_{bd} is the inhibition constant that describes the alternative pathway of release of Q from EQB and is defined as k_7k_{12}/k_9k_{11}. The normal release of Q is represented by k_7, which is actually a net rate constant (Cleland, 1975), composed of the three steps comprising the ordered release of Q.

Kinetics of Dead-End Inhibitors. Noncompetitive and uncompetitive inhibition by neomycin C show that this dead-end inhibitor binds to two forms of enzyme. The linear effect on the slopes of the inhibitor versus aminoglycoside (Figure 6) indicates competition between substrate and inhibitory aminoglycosides for EA, the Mg–ATP–enzyme complex. But the uncompetitive inhibition versus nucleotide (Figure 7) at a high, fixed concentration of aminoglycoside requires that the inhibition in this pattern arises from combination of neomycin C with a form of enzyme separated from Mg–ATP binding by irreversible steps (Cleland, 1963), which must be the enzyme–AMP–aminoglycoside complex. Secondary binding of neomycin C with this form of enzyme will also account for the intercept effect versus gentamicin A (Figure 6), and because the inhibition is also partial, Q can escape from an EQI complex as well as from EQB, but again at a slower rate than from EQ. A mechanism for this form of dead-end inhibition is illustrated in Scheme II and described by the equation:

$$\frac{v}{E_t} = \frac{VAB}{K_{ia}K_b + K_bA(1 + I/K_{is}) + K_aB + \dfrac{AB(1 + I/K_{ii})}{1 + I/K_{id}}} \quad (15)$$

where the definitions of the inhibition constants are $K_{is} = k_{14}/k_{13}$, $K_{ii} = k_{18}/k_{17}$, and $K_{id} = k_7k_{18}/k_{15}k_{17}$.

Kinetics of Multiple Substrate and Dead-End Inhibition. The similarity between Schemes I and II leads to the prediction that substrate inhibition and secondary dead-end inhibition should have a competitive component versus each other. To test this prediction and to confirm the origin of partial kinetic patterns, the dead-end inhibition by neomycin C versus tobramycin was examined in greater detail. For mutually exclusive inhibitors, increasing concentrations of one raises the apparent inhibition constant of the other according to a linear

Scheme III: Combined Substrate and Dead-End Inhibition

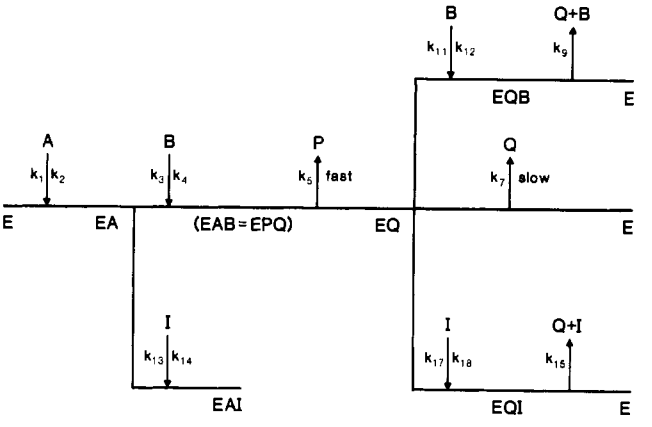

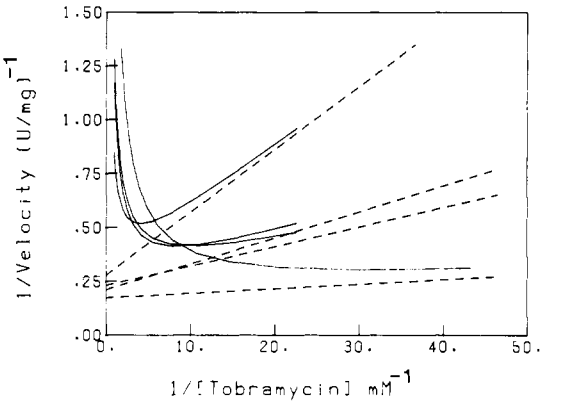

FIGURE 10: Intercept region of multiple inhibition pattern in Figure 5.

function, but for antagonistic yet not exclusive inhibitors, the increase is hyperbolic. Apparent substrate inhibition constants for tobramycin versus increasing concentrations of neomycin C give a linear fit in support of mutually exclusive binding (see legend to Figure 5, plot not shown).[4]

A mechanism for multiple inhibition by tobramycin (B) and neomycin C (I) is illustrated by Scheme III and described by the equation:

$$\frac{v}{E_t} = VAB/\left[K_{ia}K_b + K_bA(1 + I/K_{is}) + K_aB + \frac{AB(1 + B/K_{bi} + I/K_{ii})}{1 + B/K_{bd} + I/K_{id}} \right] \quad (16)$$

where K_{is}, K_{bi}, K_{ii}, K_{bd}, and K_{id} have the same values as described above. The competitive component of multiple inhibition is the mutually exclusive binding of B and I to EQ, to form EQB and EQI, respectively. The origins of partial substrate inhibition and the partial component of dead-end inhibition are similar; both originate from an escape of Q from these ternary complexes. Although hyperbolic intercept effects could not be discerned in the pattern of multiple inhibition, partial inhibition was inferred from the replots of data gathered

[4] This is simply a restatement of the postulates of Yonetani and Theorell (1964) and can be easily demonstrated by the construction of secondary plots from patterns of doubly inhibited velocities. If the binding of two inhibitors were mutually exclusive, a parallel pattern of lines should obtain. However, the presence of parallel lines can only be discerned with straight lines; because the lines obtained with partial inhibitors are curved, the question of a parallel attribute could not be addressed directly and it became necessary to find a geometric derivative of this kinetic question. The effect of one inhibitor on the *inhibition constant* of the other is such a derivative.

when the inhibitors acted alone. This inference was confirmed when the doubly inhibited data were examined by a computer-assisted enlargement of the intercepts region of the fitted lines of Figure 5, as shown in Figure 10. Obscured at the scale of the original figure are intersections of the solid, substrate-inhibited lines, showing that neomycin C causes activation of the substrate-inhibited enzyme. Because "activation" by an "inhibitor" can only occur if the inhibition is partial and the binding of the inhibitor diverts the enzyme from a slower to a faster pathway, it follows that activation of ANT(2″)-I by neomycin arises because the rate of release of Q from EQI is faster than from EQB.

Kinetics of Product Inhibition. For enzymes obeying a normal Theorell–Chance kinetic mechanism, product inhibition by Q ought to be competitive against A because Q and A compete for free enzyme. Therefore, the pronounced noncompetitive inhibition by AMP–tobramycin at K_m levels of Mg–ATP (Figure 7) requires two reconciliations. First, the large intercept effect requires that AMP–tobramycin engage in secondary binding to another form of enzyme and not simply compete with Mg–ATP for free enzyme. Given the secondary bindings of substrates and dead-end inhibitors to EQ, binding of a second Q to form EQQ seems likely. This mode of inhibition arises from binding of the antibiotic portion of the AMP–tobramycin molecule to the exposed aminoglycoside binding site of the EQ complex. Second, the small slope effect suggests weak binding of AMP–tobramycin to free enzyme, in seeming contradiction to the near-total dependence of V on its release and regeneration of free enzyme. Moreover, AMP–tobramycin resembles multisubstrate analogue inhibitors which have dissociation constants much less than either component alone, frequently in the nanomolar range. In contrast, the K_{is} for AMP–tobramycin is an order of magnitude greater than the K_{is} of neomycin or K_{ii} of tobramycin. The explanation for this seeming contradiction came unexpectedly from the results of pH- and viscosity-dependent kinetics discussed in the following paper (Gates & Northrop, 1988b) which require that the aminoglycoside portion of Q be released prior to the release of pyrophosphate, product P.

Kinetics of Multiple Product and Dead-End Inhibition. Northrop and Cleland (1974) devised a test for secondary binding of inhibitors to an EQ complex by arguing that an enhancement of this mode of inhibition should follow the addition of product to reaction mixtures because added Q increases steady-state levels of EQ available for secondary binding. During studies of NAD-specific isocitrate dehydrogenase, a negative result was obtained in which the addition of $NADP^+$ failed to cause an enhancement of substrate inhibition by α-ketoglutarate, providing kinetic evidence that α-ketoglutarate was actually binding to the central complex in a random kinetic mechanism, and not to EQ in an ordered one. In a later application of the test, Rife and Cleland (1980) obtained a positive result in which the addition of $NADP^+$ enhanced substrate inhibition of glutamate dehydrogenase from α-ketoglutarate by increasing the steady-state level of the enzyme–$NADP^+$ complex in an ordered mechanism.

The present results differ from both cited precedents because of the unique characteristic of the Theorell–Chance kinetic mechanism: during steady-state turnover, by definition, virtually all of the enzyme already exists as EQ. Consequently, the steady-state level of EQ cannot be increased by adding Q to assay mixtures. Moreover, because Q can bind to EQ in this instance, increasing concentrations of product actually decrease substrate inhibition, as evidenced by an increase in the apparent substrate inhibition constants of tobramycin with increasing neomycin C (see legend to Figure 9).

Formation of an Enzyme–Substrate Abortive Complex. The mechanism for partial substrate inhibition illustrated in Scheme I implies the formation of an EB complex after the release of Q from the EQB complex. Questions arise as to whether EB also can be formed by direct binding of the second substrate to free enzyme, and if so, whether this additional reaction pathway is kinetically significant. That EB can be formed from free enzyme under equilibrium conditions was demonstrated during chromatographic purification of ANT-(2″) because the enzyme bound to aminoglycoside-linked agarose affinity resins in the absence of nucleotide (Van Pelt & Northrop, 1984). Therefore, the complete mechanism of ANT(2″) must accommodate the formation of an abortive substrate complex. The rate equation for a steady-state, abortive substrate complex mechanism is

$$v = \frac{VAB}{K_bA + K_aB(1 + B/K_d) + K_{ia}K_b(1 + B/K_d) + AB} \quad (17)$$

where K_d is the dissociation constant of EB. Two terms from eq 13 are altered by this dissociation constant, K_a and $K_{ia}K_b$. Equation 17 predicts substrate inhibition by B that is competitive with A, because of the modified K_a term. The lack of a slope effect in Figures 3 and 4 implies an absence of this competitive component, ruling out a steady-state formation of an EB complex, but not a rapid-equilibrium formation, because the latter does not express a K_a term. Instead, the presence of an abortive substrate complex in a rapid-equilibrium ordered mechanism alters only the $K_{ia}K_b$ term, giving an equation rearranged to resemble eq 13 as

$$v = \frac{VAB}{K_bA + K_{ia}K_bB/K_d + K_{ia}K_b + AB} \quad (18)$$

Thus, the abortive complex replaces the missing K_a term with a modified $K_{ia}K_b$ term, a change that could not be detected by these experiments, and is therefore compatible with the data. Friedan (1976) reported that initial velocity and product inhibition patterns for the abortive rapid-equilibrium ordered mechanism are identical with the patterns obtained from a normal rapid-equilibrium random mechanism (cf. eq 13 and 18); hence, these two kinetic mechanisms cannot be distinguished by the usual kinetic methods, but orderedness in the binding of substrates can still be detected by the alternative substrate diagnostic. The limitations of this important distinction is examined elsewhere (Gates & Northrop, 1988c).

Significance of the Kinetic Mechanism. The Theorell–Chance mechanism was first proposed to explain product inhibition of horse liver alcohol dehydrogenase (Theorell & Chance, 1951). The mechanism is a variant of the ordered Bi Bi reaction (Cleland, 1963) in which turnover is controlled by release of the second product. Initially, the dehydrogenase reaction was perceived to be so extreme that hydride transfer was throught to occur independently of any central complex. However, it has since been demonstrated that central complexes do exist in the alcohol dehydrogenase catalyzed reaction and that although the reaction is predominantly ordered, there is some degree of randomness of substrate and product binding (Wratten & Cleland, 1963, 1965). More recently, rabbit muscle lactate dehydrogenase and purine nucleoside phosphorylase were also shown by product inhibition kinetics to follow Theorell–Chance kinetic mechanisms (Lewis, 1977; Lewis & Lowy, 1979; Zewe & Fromm, 1962). Similarly, choline acetyltransferase follows a predominantly ordered Theorell–Chance mechanism as assessed by dead-end inhib-

ition kinetics and equilibrium isotope exchange (Hersh & Peet, 1977; Hersh, 1982). Milman et al. (1980) reported a complex hybrid mechanism for asparagine synthetase, consisting of a two-site ping-pong segment and a Theorell–Chance sequential segment. Using different viologen dyes as the reducing substrate, Morpeth and Boxer (1985) postulated that nitrate reductase follows a Theorell–Chance mechanism. Such investigations need corroborative evidence, and the results presented in the following paper (Gates & Northrop, 1988b) demonstrate that variation of kinetic constants with viscosity and pH may serve as a useful means for corroboration.

Significance of Kinetics to Antibiotic Resistance. The results of this kinetic analysis show that ANT(2″)-I follows a more extreme mechanism than that suggested by Lombardini and Cheng-Chu (1980). Its rate of turnover is thousands of fold less than the net rate of catalysis, which raises the serious question of how the enzyme confers resistance to bacteria after its first encounter with antibiotic, because the natural substrates appear to be suicide substrates in that they generate very tight-binding products. The answer to this paradox is that the self-generated inhibition affects V and turnover but does not affect V/K_b. Separate experiments have established a 99.9% correlation between antibiotic resistance in the parent R factor bacteria and V/K_b values of isolated ANT(2″)-I (C. A. Gates, and D. B. Northrop, unpublished results). Thus, what is critical to antibiotic resistance is the apparent rate of *apprehension* of antibiotics as they enter the bacterial cell, not the subsequent rate of *inactivation* of antibiotics. This is a very subtle kinetic distinction with very important implications to the design and synthesis of new antimicrobial compounds.

ACKNOWLEDGMENTS

We thank Kesavan Radika for helpful discussions and assistance with the manuscript and W. Wallace Cleland for assistance with the derivation of rate equations describing partial inhibition.

REFERENCES

Barman, T. E. (1969) *Enzyme Handbook*, Vol. I, pp 491–494, Springer-Verlag, New York, NY.

Cleland, W. W. (1963) *Biochim. Biophys. Acta 67*, 188–196.

Cleland, W. W. (1975) *Biochemistry 14*, 3220–3224.

Duggleby, R. G. (1984) *Comput. Biol. Med. 14*, 447–455.

Friedan, C. (1976) *Biochem. Biophys. Res. Commun. 68*, 914–917.

Gates, C. A., & Northrop, D. B. (1984) *Fed. Proc., Fed. Am. Soc. Exp. Biol. 43*, 1874.

Gates, C. A., & Northrop, D. B. (1985) *Fed. Proc., Fed. Am. Soc. Exp. Biol. 44*, 1810.

Gates, C. A., & Northrop, D. B. (1988a) *Biochemistry* (preceding paper in this issue).

Gates, C. A., & Northrop, D. B. (1988b) *Biochemistry* (following paper in this issue).

Gates, C. A., & Northrop, D. B. (1988c) *Biochem. Biophys. Res. Commun. 152*, 406–410.

Goldman, P. R., & Northrop, D. B. (1975) *Biochem. Biophys. Res. Commun. 66*, 1408–1413.

Hersh, L. B. (1982) *J. Biol. Chem. 257*, 12820–12825.

Hersh, L. B., & Peet, M. (1977) *J. Biol. Chem. 252*, 4796–4802.

Lewis, A. S. (1977) *J. Biol. Chem. 252*, 732–738.

Lewis, A. S., & Lowy, B. A. (1979) *J. Biol. Chem. 254*, 9927–9932.

Lombardini, J. B., & Cheng-Chu, M. (1980) *Int. J. Biochem. 12*, 427–431.

Martel, A., Masson, M., Moreau, N., & LeGoffic, F. (1983) *Eur. J. Biochem. 133*, 515–521.

Milman, H. A., Cooney, D. A., & Huang, C. Y. (1980) *J. Biol. Chem. 255*, 1862–1866.

Morpeth, F. F., & Boxer, D. H. (1985) *Biochemistry 24*, 40–46.

Norris, S. M., & Raudin, J. I. (1984) *Infect. Control 5*, 188–191.

Northrop, D. B., & Cleland, W. W. (1974) *J. Biol. Chem. 249*, 2928–2931.

Pelletier, L. L. (1985) *IC, Infect. Control 6*, 226–230.

Radika, K., & Northrop, D. B. (1984a) *Biochemistry 23*, 5118–5122.

Radika, K., & Northrop, D. B. (1984b) *Anal. Biochem. 141*, 413–417.

Radika, K., & Northrop, D. B. (1984c) *J. Biol. Chem. 259*, 12543–12546.

Rife, J. E., & Cleland, W. W. (1980) *Biochemistry 19*, 2321–2328.

Theorell, H., & Chance, B. (1951) *Acta Chem. Scand. 5* (*Suppl.*), 1127–1144.

Van Pelt, J. E., & Northrop, D. B. (1984) *Arch. Biochem. Biophys. 230*, 250–263.

Williams, J. W., & Northrop, D. B. (1978) *J. Biol. Chem. 253*, 5902–5907.

Wratten, C. C., & Cleland, W. W. (1963) *Biochemistry 2*, 935–941.

Wratten, C. C., & Cleland, W. W. (1965) *Biochemistry 4*, 2442–2451.

Yonetani, T., & Theorell, H. (1964) *Arch. Biochem. Biophys. 106*, 243–251.

Zewe, V., & Fromm, H. J. (1962) *J. Biol. Chem. 237*, 1668–1675.